Source Location of Forced Oscillations based on Bus Frequency Measurements

Álvaro Ortega
Instituto de Investigación Tecnológica, ICAI
Universidad Pontificia Comillas
Madrid, Spain
aortega@comillas.edu
ORCID iD: 0000-0001-5749-0678

Federico Milano
School of Electrical and Electronic Engineering
University College Dublin
Dublin, Ireland
federico.milano@ucd.ie
ORCID iD: 0000-0002-0049-9185

***Abstract*—The paper proposes a technique to locate the source of forced oscillations in power systems. The only requirement is the availability of bus frequency measurements as obtained, for example, from phasor measurement units. The proposed technique is model-agnostic, optimization-free, non-confidential, and independent from the source and the frequency of the forced oscillations. Accuracy and robustness with respect to noise are demonstrated through two examples based on the IEEE 14-bus and New England 39-bus systems, as well as a case study based on a 1,479-bus dynamic model of the all-island Irish transmission system.**

***Index Terms*—Forced oscillation (FO), frequency estimation, phasor measurement unit (PMU), discrete sine transform (DST).**

I. Introduction

Forced oscillations (FOs) in power systems result from external periodic perturbations as opposed to *natural* or *free* oscillations that are originated from the coupling of power system devices. While the latter can be generally damped by means of control actions, FOs are usually suppressed by disconnecting their source. It is thus crucial for system operators to reliably and swiftly locate FOs in order to prevent potential cascading phenomena.

References [1] and [2] provide detailed reviews of available techniques to locate the source of FOs. All the approaches discussed in [1], [2] and in the references therein show some relevant drawback, such as: (i) the need of detailed information of the models [3], [4]; (ii) unfitness for large systems [5]; (iii) applicability only to post-fault analysis studies [4]; (iv) inability to identify the source of FOs in a wide range of frequencies [6]; and (v) inability to cope with sources of different nature [7]. A recent promising approach to locate FOs is proposed in [8], where a multi-stage optimization algorithm is proposed, which can cope with parameter uncertainties in real-time applications. In [8], however, the authors do not tackle the issue of the scalability of the technique proposed, and they focus only on generators as the source of the FOs in a rather narrow range of frequencies of the FOs, namely from 0.5 to 0.86 Hz, while the typical range of frequencies FOs spans a quite wider interval, namely from 0.12 to 14 Hz.

This work was supported by the European Commission, by funding Á. Ortega under Grant No. 883985 and F. Milano under Grant No. 883710. F. Milano is also funded by Science Foundation Ireland, through project AMPSAS, Grant No. SFI/15/IA/3074.

Several references, including recent works, have made use of Fourier-related transforms and indices such as the Power Spectral Density (PSD) applied to measurement signals from Phasor Measurement Units (PMUs) for the detection of FOs, e.g., [9]–[12]. These references are aimed at detecting the presence of FOs, not to identify the location of their sources. The possibility to use the PSD to estimate the location of the FOs source is illustrated in [1] through voltage signals. The approach above shows low accuracy when FOs are characterized by frequencies that are relatively low or close to system natural modes. Another approach to locate FOs based on PMU measurement is described in [13], where the sources are identified by means of the concept of dissipating energy flows (DEFs). DEF-based approaches, however, require the assumptions that FOs are originated by synchronous machines, lossless network and constant power loads.

This paper proposes a technique to estimate the location of the source of FOs based on a byproduct of the Frequency Divider Formula (FDF) originally presented by the authors in [14], and on the processing of the resulting signals through the well-known Discrete Sine Transform (DST). Thanks to the features of the FDF, the proposed technique is:

- *Model-agnostic*, as one does not need to know anything about the device that originates FOs, nor about any other system dynamics, since only information about the system topology is required;
- *Optimization-free*, as the estimation of the FO source is based on the direct processing of PMUs data;
- *Non-confidential*, as it only requires bus frequency measurements, which can be readily obtained with PMUs;
- *Independent from the source and frequency of the FOs*, being reliable for any source and in the typical FO frequency range; and
- *Scalable*, as it is suitable for large electrical networks (thousands of buses).

The paper is organized as follows. The methodology of the proposed approach is formulated and duly discussed in Section II. A set of illustrative examples based on two well-known benchmark networks is presented in Section III. Section IV discusses a case study based on the detailed dynamic, 1,479-bus model of the All-island Irish Transmission System. Finally, Section V draws conclusions and future work directions.

II. Methodology

The objective of this section is to derive an expression of the harmonic "frequency injections", called $\boldsymbol{\alpha}$ in the remainder of this work, and their link with the frequency variations $\Delta\boldsymbol{\omega}$ at the buses of the grid.

We derive these expressions in two ways. First Section II-A shows that the time derivative of the current injection at buses is linked to bus frequency variations. This fact indicates that the FO harmonic sources and bus frequency variations are, as expected, intertwined. Then, Section II-B shows that the obtained expression is, in fact, an extension of the FDF. This observation allows stating the equivalence of FO harmonic injections to the variations of frequency during an electromechanical transient. Finally, Section II-C presents the proposed technique to locate the FO sources.

A. Link between Current Injections and Bus Frequencies

Let us consider the current injections at the network buses as a function of the network admittance matrix and the bus voltages:

$$\bar{\boldsymbol{\imath}}(t) = \bar{\mathbf{Y}}_{\mathrm{bus}}\,\bar{\boldsymbol{v}}(t)\,, \tag{1}$$

where $\bar{\boldsymbol{\imath}}$ and $\bar{\boldsymbol{v}}$ are assumed to be quasi-steady state phasors. Then, let us apply to (1) common simplifications utilized in transient stability analysis, namely, (i) the elements of the admittance matrix are constant, i.e., their dependency on the frequency can be neglected, except for discrete events such as line outages; and (ii) the resistance of the transmission lines are negligible compared with their reactances, thus:

$$\bar{\mathbf{Y}}_{\mathrm{bus}} \approx j\mathrm{Im}\{\bar{\mathbf{Y}}_{\mathrm{bus}}\} = j\mathbf{B}_{\mathrm{bus}}\,. \tag{2}$$

We then calculate the time derivative of (1), assuming that the derivatives of the bus voltages can be approximated as:

$$\frac{d}{dt}\bar{\boldsymbol{v}}(t) \approx j\Delta\boldsymbol{\omega}(t)\circ\bar{\boldsymbol{v}}(t)\,, \tag{3}$$

where $\circ$ indicates the element-by-element product and $\Delta\boldsymbol{\omega} = \boldsymbol{\omega} - \omega_s\mathbf{1}_n$ is the vector of frequency variations at the n network buses, with ω_s the fundamental (synchronous) angular frequency of the system, e.g., 314.16 rad/s for a 50 Hz system. The approximation of the time derivative of the bus voltages in (3) is fully justified in the context of electromechanical transients as thoroughly discussed in [14] but is also perfectly consistent with the typical range of frequencies of FOs, which, as discussed in Section I, span a range from 0.12 to 14 Hz.

With these assumptions, the time derivative of (1) can be written as:

$$\frac{d}{dt}\bar{\boldsymbol{\imath}}(t) \approx j\mathbf{B}_{\mathrm{bus}}\Delta\boldsymbol{\omega}(t)\circ\bar{\boldsymbol{v}}(t)\,, \tag{4}$$

and, dividing element-by-element by $j\bar{\boldsymbol{v}}$:

$$\boxed{\boldsymbol{\alpha}(t) = \frac{d}{dt}\bar{\boldsymbol{\imath}}(t) \div [j\bar{\boldsymbol{v}}(t)] \approx \mathbf{B}_{\mathrm{bus}}\Delta\boldsymbol{\omega}(t)}\,, \tag{5}$$

where $\div$ is the element-by-element division between two vectors. Equation (5) is the sought expression that links the time derivative of harmonic current injections with frequency variations in the network.

As a consequence of the assumptions utilized to obtain (5), the right hand side of (5) is real, hence also the elements of $\boldsymbol{\alpha}$ are real. Moreover, (5) has the same structure as (1), meaning that bus frequency variations $\Delta\boldsymbol{\omega}$ are "potentials", whereas $\boldsymbol{\alpha}$ are "flows". This observation is reprised in Section II-C and is key for the proposed technique to locate the sources of FOs.

B. Equivalence of FOs and Electromechanical Transients

The expression in (5) is utilized in this paper to determine the sources of FO. The derivation given so far, however, does not justify the physical meaning of the vector $\boldsymbol{\alpha}$, which is, in turn, that of a "current source" of frequency variations at buses. To clarify this point, we utilize the concept of FDF.

The FDF originally proposed in [14] can be written as:

$$\mathbf{B}_{\mathrm{G}}\Delta\boldsymbol{\omega}(t) - \mathbf{B}_{\mathrm{BG}}\Delta\boldsymbol{\omega}_r(t) = \mathbf{B}_{\mathrm{bus}}\Delta\boldsymbol{\omega}(t)\,. \tag{6}$$

where $\Delta\boldsymbol{\omega}$ has the same meaning as in (1); $\Delta\boldsymbol{\omega}_r = \boldsymbol{\omega}_r - \omega_s\mathbf{1}_m$ is the vector of the frequency variations of the rotor speeds of the m synchronous machines; $\mathbf{B}_{\mathrm{G}}$ is a diagonal matrix whose i-th diagonal element is non-zero if there is a synchronous machine connected to bus i and its value is the inverse of the machine internal reactance; $\mathbf{B}_{\mathrm{BG}}$ is the susceptance incidence matrix between generators and network buses with inclusion of the internal reactances of the synchronous machines; and $\mathbf{B}_{\mathrm{bus}}$ is the imaginary part of the standard network admittance matrix;

Comparing (6) and (5) leads necessarily to conclude that, for synchronous machines, one has:

$$\boldsymbol{\alpha}_{\mathrm{G}}(t) = \mathbf{B}_{\mathrm{G}}\Delta\boldsymbol{\omega}(t) - \mathbf{B}_{\mathrm{BG}}\Delta\boldsymbol{\omega}_r(t)\,, \tag{7}$$

that is, the "harmonic" injection of synchronous machines depends on the deviation of their rotor angular speeds with respect to the reference frequency of the system.

From (5), we can now extrapolate the concept of "generators" in a wider sense, i.e., not only synchronous machines, but actually any device that locally imposes a frequency variation, and, in particular, an FO source. The elements of $\boldsymbol{\alpha}$ can thus be interpreted as the "boundary conditions" for the bus frequencies of the grid. The vector $\boldsymbol{\alpha}$ itself can be thought as the sum of two terms, the frequency variations due to synchronous machines and those due to FOs, i.e.,

$$\boldsymbol{\alpha}(t) = \boldsymbol{\alpha}_{\mathrm{G}}(t) + \boldsymbol{\alpha}_{\mathrm{FO}}(t)\,. \tag{8}$$

C. Identification of the Location of FO Sources

The relevance of (5) in the context of this work is that it states that the effect of $\boldsymbol{\alpha}$ can be determined by measuring bus frequency variations and properly weighting such variations with the elements of the matrix $\mathbf{B}_{\mathrm{bus}}$. This property of the FDF has been exploited in [15] to estimate the rotor speed of synchronous machines and in [16] and [17] to quantify the frequency support and inertial response provided by non-synchronous devices, respectively.

Here, we propose another application of such a property, namely, to study the frequency spectrum of the elements of $\boldsymbol{\alpha}$ to determine where the FO is located. With this aim, let

us assume a stationary condition where each AC voltage of the system oscillates with the fundamental frequency ω_s and a constant FO with angular frequency $\omega_{\rm FO}$. Then, the expression (5) becomes:

$$\begin{aligned}\boldsymbol{\alpha}(t) &= \mathbf{B}_{\rm bus}\big(\omega_s \mathbf{1}_n + \boldsymbol{a}_{\rm FO} \circ \sin(\omega_{\rm FO} t + \boldsymbol{\phi}_{\rm FO}) - \omega_s \mathbf{1}_n\big) \\ &= \mathbf{B}_{\rm bus}\big(\boldsymbol{a} \circ \sin(\omega_{\rm FO} t + \boldsymbol{\phi})\big)\,,\end{aligned} \tag{9}$$

where the vectors $\boldsymbol{a}$ ($\boldsymbol{a}_{\rm FO}$) and $\boldsymbol{\phi}$ ($\boldsymbol{\phi}_{\rm FO}$) are the amplitudes and phase shots, respectively, of the "total" (FO) harmonic at every bus of the grid. The expression (9) shows that, while in stationary conditions, the FDF "sees" the harmonics as time-dependent periodic variations with respect to the fundamental frequency ω_s.

If the system includes a set of harmonics, say Ω_i, then (9) becomes:

$$\boldsymbol{\alpha}(t) = \mathbf{B}_{\rm bus} \sum_{i \in \Omega_i} \boldsymbol{a}_i \circ \sin(\omega_i t + \boldsymbol{\phi}_i)\,. \tag{10}$$

Both (6) and (10) state that the amplitude of frequency variations in a grid follow the same behavior of voltages in a resistive DC circuit. In a resistive circuit, the voltage at the source is always greater than at the load. Since the network is interconnected, all bus frequencies "see" the FO injected at bus i, but its effect is more evident the closer the bus is (electrically) to the location of the FO. It has to be expected, thus, that if the i-th element of vector $\boldsymbol{\alpha}_{\rm FO}$ is non-null, the frequency variations due to the FO will impact mostly the i-th element of $\mathbf{B}_{\rm bus}\Delta\boldsymbol{\omega}$. Moreover, being (10) a linear expression, the superposition principle holds, and hence each harmonic can be considered to be independent from the others.

These two concepts together lead to the following proposition. The i-th element of the vector of amplitudes $\boldsymbol{a}_{\rm FO}$ corresponding to the i-th bus where the FO is injected into the grid is independent from other harmonics and, being equivalent to a voltage source in a resistive circuit, is greater than the other elements in the same vector.

In the vast majority of cases, FOs are characterized by a single constant fundamental frequency, $\omega_{\rm FO}$ as in (9). Hence, a well-known Fourier-related transform widely used in harmonic analysis, namely the Discrete Sine Transform (DST), is used to process the right-hand side of (5) as follows [18]:

$$\begin{aligned}\hat{\alpha}_i\{k\,\omega_o\} =& \frac{2}{N}\sum_{n=0}^{N-1} \alpha_i[n\Delta t]\sin(k\,\omega_o n\Delta t)\ , \\ & k = 0, 1, 2, \ldots, N-1\ ,\end{aligned} \tag{11}$$

where Δt and N are the sampling time and the number of samples of the time series, respectively; $\omega_o = 2\pi/T_o$ with $T_o = N\Delta t$; and α_i is the sampled signal at bus i, given by:

$$\alpha_i[n\Delta t] = \mathbf{B}_{{\rm bus},i}\,\boldsymbol{\omega}[n\Delta t]\ , \tag{12}$$

where $\mathbf{B}_{{\rm bus},i}$ is the i-th row of matrix $\mathbf{B}_{\rm bus}$. Note also that, due to the sparsity of the network susceptance matrix $\mathbf{B}_{\rm bus}$, the number of frequency measurements required to estimate the i-th element of the vector $\boldsymbol{\alpha}$ is small, as one only needs to measure the frequency at bus i, and its adjacent buses (see also the discussion in [15]).

Two remarks on the proposed technique are relevant. First, the assumption of stationarity conditions is not crucial for the validity of (5), and hence (9), but are assumed here to simplify the Fourier analysis discussed above. If the FO has a transient behavior as discussed in the example [13], a DFT with mobile window as commonly implemented in PMUs can be utilized. As a second remark, in the literature, the DFT of several other quantities, e.g., power flows and bus voltages, have been considered for the identification of the locations of the sources of FOs. None of these quantities, however, is a linear combination of the frequency variations of the buses as the vector $\boldsymbol{\alpha}$. This is the feature that makes the approach proposed in this paper particularly adequate for the identification of FO sources. This point is thoroughly illustrated and discussed in the following sections.

III. Examples

The proposed approach to estimate the location of the source of forced oscillations in a transmission grid is first illustrated by means of two well-known benchmark networks used for dynamic analysis, namely the IEEE 14-bus and the New-England 39-bus test systems, in Subsections III-A and III-B, respectively.

Uncorrelated stochastic processes of the loads are utilized to model load volatility. Unless otherwise indicated, the Ornstein-Uhlenbeck process (mean-reverting) [19], is considered for all loads of the systems discussed in this section as well as in the case study of Section IV. PMUs used to measure the bus frequencies are modeled as Synchronous Reference Frame Phase-Locked Loops (SRF-PLLs). For all scenarios, time domain simulations last 600 s, with a time step of 20 ms.

The simulation tool used in the examples of this section, as well as in the case study of Section IV is Dome [20]. The simulations were executed on a 64-bit Linux Ubuntu 18.04 operating system running on an 8-core 3.40 GHz Intel© Core i7™ with 16 GB of RAM.

A. IEEE 14-bus system

The description and data of this benchmark system are provided in [21].

In this example, FOs have been applied, individually and in separate simulations, to the mechanical power of the synchronous machines at buses 1 and 2, as well as to the active power consumption of all loads, which are connected to all buses except for 1, 7 and 8. All FOs have a frequency $\omega_{\rm FO}$ of 0.5 Hz, and their amplitude is proportional to either the capacity of the machine (2%), or to the active power load consumption (10%).

1) Active Power-Driven Forced Oscillations: Figure 1 shows the trajectories of the elements of vector $\boldsymbol{\alpha}$ and their respective DSTs for the case where the FOs are injected by the machine at bus 1. By processing $\boldsymbol{\alpha}$ signals by means of the DST, one can estimate the location of the source of the FOs by analyzing the peak values observed at the frequency

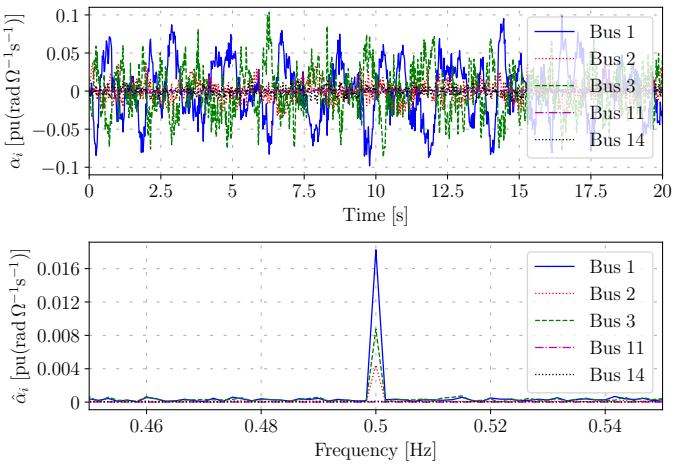

Fig. 1. IEEE 14-bus system – Trajectories of the elements of vector $\boldsymbol{\alpha}$ and their respective DSTs when FOs are applied to the mechanical power of the synchronous machines at bus 1.

of such oscillations. As anticipated in Section II, the highest peak corresponds to the bus where the FOs originate. This is also shown in Fig. 2 for the cases of the two synchronous generators, and four loads at buses 2, 3, 11 and 14. Figure 2 shows the values $\hat{\boldsymbol{\alpha}}\{\omega_{\text{FO}}\}$ of the buses to which a device is connected (either generator, compensator or load). These values are normalized as follows:

$$\langle \hat{\alpha}_i \rangle = \frac{\hat{\alpha}_i\{\omega_{\text{FO}}\}}{\max(\hat{\boldsymbol{\alpha}}\{\omega_{\text{FO}}\})} \,. \tag{13}$$

For all cases studied, the bus with the highest peak corresponds to the source of the FOs.

2) Voltage-Driven Forced Oscillations: To illustrate that the nature of the source of FOs does not affect the accuracty of the results, Fig. 3 shows the values of $\langle \hat{\alpha}_i \rangle$ at $\omega_{\text{FO}} = 0.5$ Hz when the oscillations are originated by the Automatic Voltage Regulators (AVRs) of the machines at buses 1 and 2. These oscillations can be captured accurately by the proposed approach. An oscillation originated by an AVR, in fact, introduces oscillations in all variables of a synchronous machine and, thus, also in the rotor speed of the machine.

3) Spectrum Overlapping: The next scenario discussed in this Section considers the case when the frequency of the FOs overlaps with that of the electromechanical modes of the synchronous machines. Figure 4 shows the values of $\langle \hat{\alpha}_i \rangle$ at $\omega = 1.45$, 1.5 and 1.55 Hz when FOs ($\omega_{\text{FO}} = 1.5$ Hz) are applied to the active power consumption of the load at bus 11. It can be seen that, while the electromechanical modes of the machines span a range of frequencies around 1.5 Hz, the FOs are localized at a very narrow range around ω_{FO}. This property of FOs allows estimating their source even when their ω_{FO} overlaps with other oscillating modes of the system that can even show higher values of $\langle \hat{\alpha}_i \rangle$.

4) Natural Oscillations: The last scenario discussed in this section considers the 20% overload of the IEEE 14-bus system, with the loads modeled as constant PQ. Under this conditions, the system can show undamped natural oscillations due to a pair of complex conjugate eigenvalues with positive real part. In this scenario, the contingency that triggers the limit cycle is the outage of the line connecting buses 2 and 4 and the results of the DST at the oscillatory frequency are shown in Fig. 5. The synchronous generator at bus 1 is the most susceptible to such oscillations. Indeed, the pair of complex eigenvalues that crosses the complex plain imaginary axis is associated with the AVR and stator voltage of the machine at bus 1.

A less expected result of simulation results is the high peak observed at bus 4. As stated above, the load at such a bus is modeled as a constant PQ load, thus no *active* device is connected to bus 4. Therefore, it could be expected that $\langle \hat{\alpha}_4 \rangle = 0$, and this is indeed what it can be observed if, e.g., only the active power injections at system buses are monitored. However, the ability of a load to maintain a constant power consumption requires the current to vary in order to compensate any bus voltage variations due to, e.g., the natural oscillations of the limit cycle [22]. These current oscillations, which cannot be detected if measuring the bus active power injection, are detected by the proposed $\langle \hat{\alpha}_i \rangle$.

Note that the load at bus 4 is the second largest load in the system, just behind the load at bus 2 which is connected together with a synchronous machine and thus its effect is coupled with that of the generator. Bus 4 is also, together with bus 5, the only bus with a load in the 69 kV region of the IEEE 14-bus system. However, the load at bus 5 is about an order of magnitude smaller than that at bus 4. These facts explain the high peak observed in Fig. 5 with respect to the other loads of the system.

B. New-England 39-bus system

The second example considers the New-England 39-bus, 10-machine test system [23].

Two simultaneous FOs are applied, namely to the mechanical power of the machine at bus 35 ($\omega_{\text{FO},1} = 0.5$ Hz), and to the active power consumption of the load at bus 25 ($\omega_{\text{FO},2} = 10$ Hz). Figure 6 shows the values of $\langle \hat{\alpha}_i \rangle$ at $\omega_{\text{FO},1}$ (top) and $\omega_{\text{FO},2}$ (bottom) for all buses where either a machine or a load is connected. The proposed approach is able to accurately estimate the source location of both FOs, despite being of different nature (generation vs. load) and with different ω_{FO}.

Note that the New England system shows a uniform and fairly symmetrical topology, whereas the IEEE 14-bus system of the previous example has all generation in the 69 kV region, and most of the load is located in the 13.8 kV region. Hence, the proposed approach shows to be accurate regardless of the topology of the grid.

IV. Case Study

To test the accuracy of the proposed approach on a large, heterogeneous system, the All-island Irish Transmission System (AIITS) is considered in this case study. The model of this grid includes 1,479 buses, 1,851 transmission lines and transformers, 245 loads, 22 conventional power plants

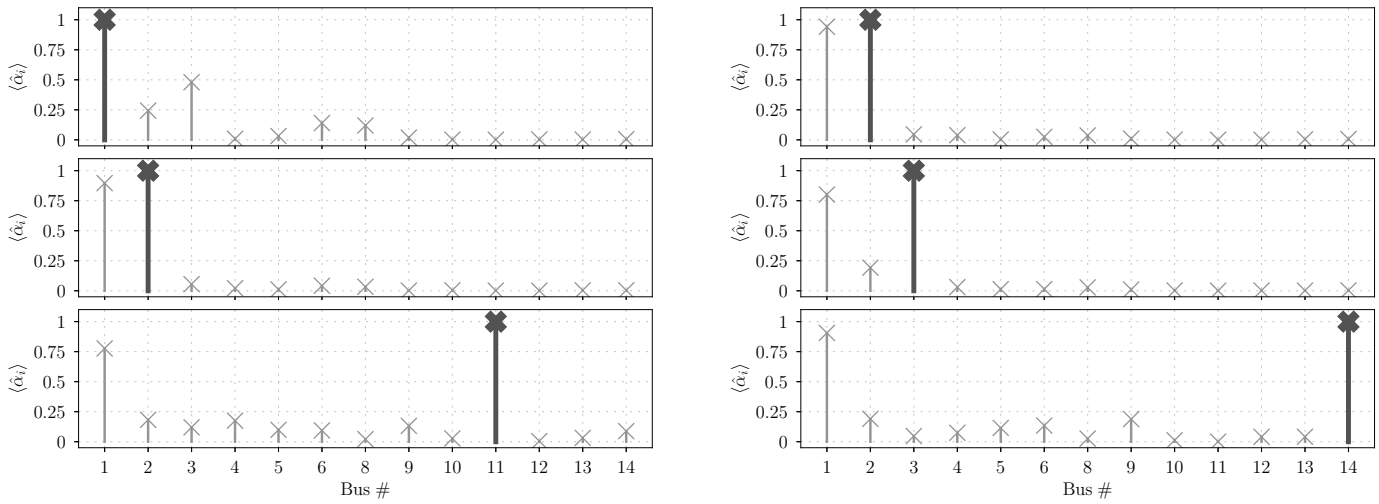

Fig. 2. IEEE 14-bus system – From left to right and from top to bottom, elements $\langle\hat{\alpha}_i\rangle$ for $\omega_{\mathrm{FO}} = 0.5$ Hz when FOs are applied to the mechanical power of the synchronous machines at buses 1 and 2, and to the active power consumption of the loads at buses 2, 3, 11 and 14.

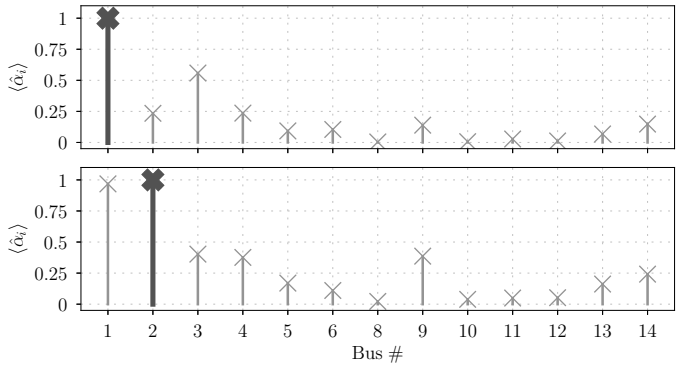

Fig. 3. IEEE 14-bus system – From top to bottom, elements $\langle\hat{\alpha}_i\rangle$ for $\omega_{\mathrm{FO}} = 0.5$ Hz when FOs are applied to the output voltage of the AVRs the synchronous machines at buses 1 and 2.

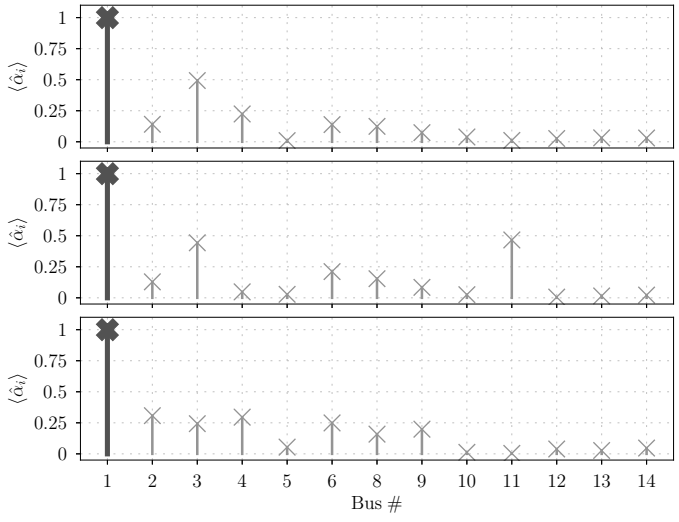

Fig. 4. IEEE 14-bus system – From top to bottom, elements $\langle\hat{\alpha}_i\rangle$ for $\omega = 1.45$, 1.5 and 1.55 Hz when FOs of $\omega_{\mathrm{FO}} = 1.5$ Hz are applied to the active power consumption of the load at bus 11.

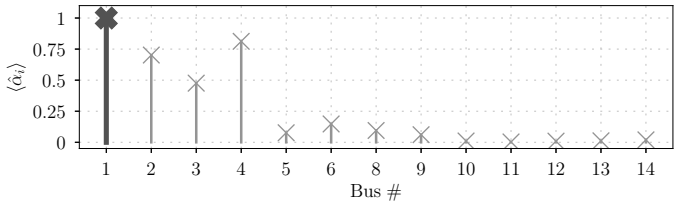

Fig. 5. IEEE 14-bus system – Elements $\langle\hat{\alpha}_i\rangle$ when a Hopf bifurcation induces a limit cycle due to the outage of the line 2-4 at 20% system overload.

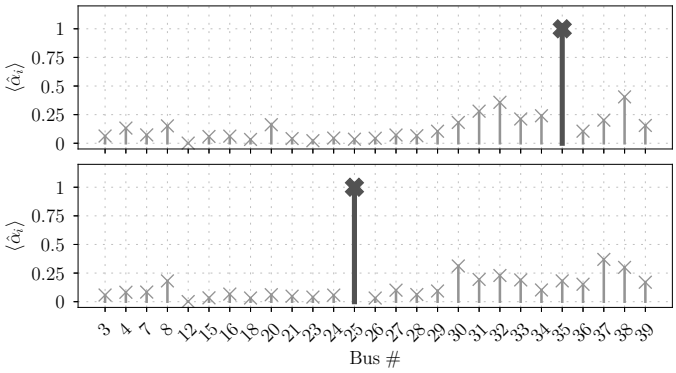

Fig. 6. New England system – Elements $\langle\hat{\alpha}_i\rangle$ for $\omega_{\mathrm{FO},1} = 0.5$ Hz (top) and $\omega_{\mathrm{FO},2} = 10$ Hz (bottom) when simultaneous FOs of different ω_{FO} are applied to the mechanical power of the synchronous machine at bus 35 and to the active power consumption of the load at bus 25.

with AVRs and Turbine Governors (TGs), six Power System Stabilizers (PSSs), and 176 Wind Power Plants (WPPs) [24].

In the simulations, apart from the load fluctuations described in the introduction of Section III, wind perturbations have also been modeled. In the long term, the stochastic process applied to the wind follows a Weibull distribution or some other non-symmetrical distribution. However, in the short term, one can approximate wind fluctuations with a Gaussian process. In this case study, the noise is modeled as a zero-average Ornstein-Uhlenbeck process.

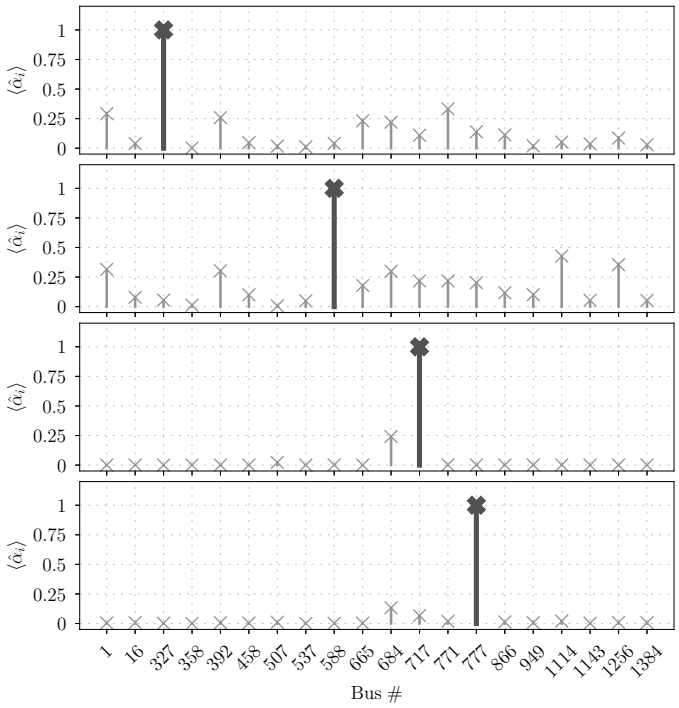

Fig. 7. AIITS – From top to bottom, a set of $\langle\hat{\alpha}_i\rangle$ when FOs are applied to the generation/loads connected to buses 327, 588, 717 and 777.

A selection of 20 buses of the AIITS are chosen to be monitored during the simulations. These buses represent synchronous generators, WPPs and loads distributed across the network. FOs with $\omega_{\rm FO} = 0.5$ Hz are applied, individually, to four of these buses.

Figure 7 shows the values $\langle\hat{\alpha}_i\rangle$ at $\omega_{\rm FO} = 0.5$ Hz of the 20 buses when FOs are applied to the mechanical torque of the WPPs at buses 327 and 588, to the mechanical power of the synchronous machine at bus 717, and to the load at bus 777. The proposed approach is able to accurately estimate the location of the FO sources despite all the external perturbations that affect the system, namely wind and load fluctuations.

V. Conclusions

This paper proposes a technique to identify the location of the source of active power/voltage phase angle-driven Forced Oscillations (FOs) based on measurements of the bus frequencies through PMUs. Simulation results based on two benchmark networks, as well as on a large real-world transmission system model, show the accuracy and reliability of the proposed approach. The technique proposed in this paper is model-independent; is suitable for any system size and topology, and for on-line applications; and can cope with a variety of types of FOs sources and frequencies.

Future work will further elaborate on the estimation of the location of FOs-induced resonances in power systems in cases where devices other than the synchronous machines are involved. Techniques to improve the accuracy of the proposed index when FOs overlap with resonance modes of the system will also be studied and developed.

References

[1] M. Ghorbaniparvar, "Survey on forced oscillations in power system," *Journal of Modern Power Systems and Clean Energy*, vol. 5, no. 5, pp. 671–682, Sep 2017.

[2] B. Wang and K. Sun, "Location methods of oscillation sources in power systems: a survey," *Journal of Modern Power Systems and Clean Energy*, vol. 5, no. 2, pp. 151–159, 2017.

[3] L. Chen, Y. Min, and W. Hu, "An energy-based method for location of power system oscillation source," *IEEE Transactions on Power Systems*, vol. 28, no. 2, pp. 828–836, 2013.

[4] J. Ma, P. Zhang, H. Fu, B. Bo, and Z. Dong, "Application of phasor measurement unit on locating disturbance source for low-frequency oscillation," *IEEE Transactions on Smart Grid*, vol. 1, no. 3, pp. 340–346, 2010.

[5] Y. Gao, D. Liu, G. Huang, and Q. Shi, "Locating method of disturbance source of forced power oscillation based on prony anyasis," in *2012 China International Conference on Electricity Distribution*, Sep. 2012, pp. 1–4.

[6] Z. Li, Y. Fang, W. Li, F. Liu, and W. Jiang, "Forced power oscillation analysis based on EEAC theory," in *2012 Asia-Pacific Symposium on Electromagnetic Compatibility*, 2012, pp. 833–836.

[7] Y. Yu, Y. Min, L. Chen, and P. Ju, "The disturbance source identification of forced power oscillation caused by continuous cyclical load," in *2011 4th International Conference on Electric Utility Deregulation and Restructuring and Power Technologies (DRPT)*, 2011, pp. 308–313.

[8] S. Chevalier, P. Vorobev, and K. Turitsyn, "A Bayesian approach to forced oscillation source location given uncertain generator parameters," *IEEE Transactions on Power Systems*, vol. 34, no. 2, pp. 1641–1649, Mar. 2019.

[9] J. Follum and J. W. Pierre, "Initial results in the detection and estimation of forced oscillations in power systems," in *2013 North American Power Symposium (NAPS)*, 2013, pp. 1–6.

[10] ——, "Detection of periodic forced oscillations in power systems," *IEEE Transactions on Power Systems*, vol. 31, no. 3, pp. 2423–2433, 2016.

[11] J. Follum, J. W. Pierre, and R. Martin, "Simultaneous estimation of electromechanical modes and forced oscillations," *IEEE Transactions on Power Systems*, vol. 32, no. 5, pp. 3958–3967, 2017.

[12] Y. Zhi and V. Venkatasubramanian, "Analysis of energy flow method for oscillation source location," *IEEE Transactions on Power Systems*, pp. 1–11, 2020, pre-print available at ieeexplore.ieee.org.

[13] S. Maslennikov, B. Wang, and E. Litvinov, "Dissipating energy flow method for locating the source of sustained oscillations," *International Journal of Electrical Power & Energy Systems*, vol. 88, pp. 55–62, 2017.

[14] F. Milano and Á. Ortega, "Frequency divider," *IEEE Transactions on Power Systems*, vol. 32, no. 2, pp. 1493–1501, Mar. 2017.

[15] F. Milano, Á. Ortega, and A. J. Conejo, "Model-agnostic linear estimation of generator rotor speeds based on phasor measurement units," *IEEE Transactions on Power Systems*, vol. 33, no. 6, pp. 7258–7268, Nov 2018.

[16] Á. Ortega and F. Milano, "A method for evaluating frequency regulation in an electrical grid part ii: Applications to non-synchronous devices," *IEEE Transactions on Power Systems*, pp. 1–10, 2020.

[17] M. Liu, J. Chen, and F. Milano, "On-line inertia estimation for synchronous and non-synchronous devices," *IEEE Transactions on Power Systems*, pp. 1–9, 2020.

[18] V. Britanak, P. Yip, and K. Rao, *Discrete Cosine and Sine Transforms*. Oxford: Academic Press, 2007.

[19] D. T. Gillespie, "Exact numerical simulation of the Ornstein-Uhlenbeck process and its integral," *Physical Review E*, vol. 54, no. 2, pp. 2084–2091, 1996.

[20] F. Milano, "A Python-based software tool for power system analysis," in *Proc. IEEE PES General Meeting*, Vancouver, BC, July 2013.

[21] S. K. M. Kodsi and C. A. Cañizares, "Modeling and simulation of IEEE 14-bus system with FACTS controllers," University of Waterloo, Waterloo, Tech. Rep. 2003-3, Mar. 2003.

[22] Á. Ortega and F. Milano, "Estimation of voltage dependent load models through power and frequency measurements," *IEEE Transactions on Power Systems*, vol. 35, no. 4, pp. 3308–3311, 2020.

[23] T. Athay, R. Podmore, and S. Virmani, "A practical method for the direct analysis of transient stability," *IEEE Transactions on Power Apparatus and Systems*, vol. PAS-98, no. 2, pp. 573–584, Mar. 1979.

[24] EirGrid Group, "All-island Irish transmission system." [Online]. Available: http://www.eirgridgroup.com